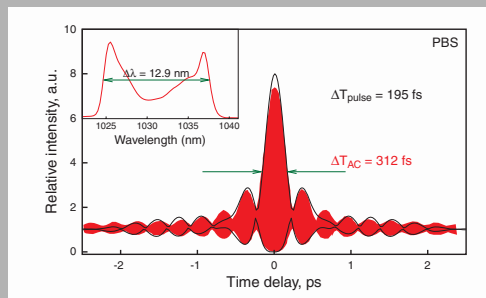


**Abstract:** Experimental results on an all-fiber, all-normal dispersion ytterbium ring laser are reported. It produces stable mode-locking of  $\sim 10$  ps pulses that can be externally compressed to as short as  $\sim 200$  fs.



Measured (red filled curves) and fitted (black lines) autocorrelation functions with the spectrum in the inset

© 2008 by Astro Ltd.  
Published exclusively by WILEY-VCH Verlag GmbH & Co. KGaA

## All-fiber, all-normal dispersion ytterbium ring oscillator

J. Fekete,<sup>1,\*</sup> A. Csérteg,<sup>2</sup> and R. Szipőcs<sup>1,3</sup>

<sup>1</sup> Research Institute for Solid State Physics and Optics, P.O. Box 49, Budapest 1525, Hungary

<sup>2</sup> Furukawa Electric Institute of Technology Ltd., 24–28, Késmárk u., Budapest 1158, Hungary

<sup>3</sup> R&D Ultrafast Lasers Ltd., P.O. Box 622, Budapest 1539, Hungary

Received: 2 September 2008, Revised: 9 September 2008, Accepted: 12 September 2008

Published online: 1 October 2008

**Key words:** fiber laser; mode-locking; ytterbium

**PACS:** 42.55.Wd, 42.60.Fc, 42.81.Gs

### 1. Introduction

Passively mode-locked fiber lasers have gained high interest because of their potentially compact, environmentally stable and alignment-free design. Although a wide variety of fiber optic components are now commercially available, they are not as reliable, and their parameters are rarely as easily controllable as that of bulk elements. This fact raises difficulties in the development of all-fiber oscillators. Much effort has been done to create all-fiber configurations [1–3], but at the ytterbium (Yb) wavelength solutions were only found lately.

Fiber lasers around  $1 \mu\text{m}$  are usually constructed with some kind of intra-cavity dispersion compensation to overcome the normal dispersion provided by the silica fibers. Free space optics, such as gratings [4] and prisms [5] as well as photonic crystal fibers [6], higher-order mode fibers [7] or chirped fiber Bragg gratings [8] have been implemented as intra-cavity dispersion compensating ele-

ments. However, for the ease of construction and use it is desirable to design fiber oscillators without any dispersion compensation.

The pulse dynamics in all-normal dispersion fiber lasers are dominated by the interplay between gain, self-phase modulation, dispersion and filtering effects. Filtering with a 10 nm bandwidth spectral filter has led to stable mode-locking of 3 nJ pulses dechirped to as short as 170 fs [9]. However, this setup employed free-space optics and such impressive results could not be reproduced by all-fiber configurations. Previous all-fiber Yb oscillators produced picosecond pulses owing to the strong spectral filtering [10], and in another approach ps pulses were generated by the pulse-shaping of the nonlinearity of a semiconductor saturable absorber mirror [11]. Lately an all-fiber similariton fiber laser was reported to produce 0.8 nJ pulses externally compressible to 627 fs [12]. This laser had a unidirectional cavity, utilizing a fiber coupled saturable Bragg

\* Corresponding author: e-mail: feketej@mail.kfki.hu

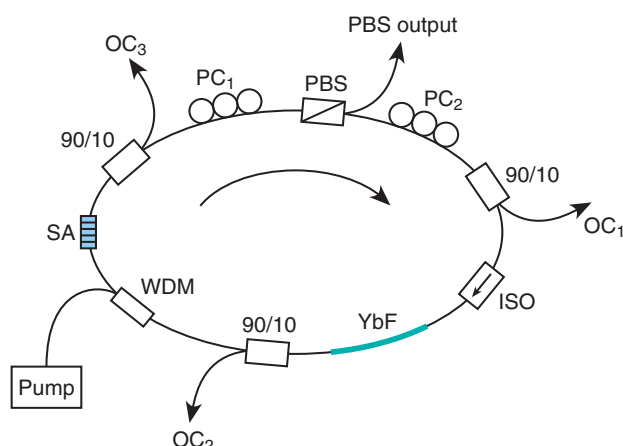


**Figure 1** (online color at [www.lphys.org](http://www.lphys.org)) Experimental setup of the laser (PBS: polarizing beam splitter; PC: polarization controller; 90/10: 90/10 splitter; OC: output coupler; ISO: isolator; YbF: Yb-doped fiber; WDM: wavelength division multiplexer; SA: saturable absorber)

reflector in a bidirectional part via a polarizing beam splitter (PBS), hence we refer to it as a  $\sigma$ -shaped resonator. Very recently, an all-fiber normal dispersion ring laser was demonstrated. It included a  $\sim 15$  nm bandwidth fiber filter, and a saturable absorber based on carbon nanotubes. The laser generated 1.5 ps, 3 nJ pulses that were compressible to 250 fs duration. However, the pedestals of the compressed pulses contained significant part of the energy because of the modulation of the spectrum [13].

In this paper we report on an all-fiber, all-normal dispersion ring oscillator where pulse-shaping is based on nonlinear polarization rotation in the fiber together with spectral and temporal filtering by a polarizing element. The laser characteristics were investigated and compared at four output ports, the rejection port of a PBS and three 90/10 splitters placed at specific positions of the oscillator. These investigations were necessary for choosing the resonator output positions optimal for the different applications. For example by removing the splitters the PBS can be used as a single output port producing relatively high quality pulses compressible to as short as 195 fs. From the practical point of view, however, a resonator including an additional output after the PBS is more promising, regarding the better pulse quality and broad unmodulated spectrum.

## 2. Experimental setup

Our purpose was to investigate the pulse characteristics at different positions in the oscillator aiming for the understanding of the pulse dynamics. For this reason we utilized several 90/10 splitters to couple out 10% of the light to measure it. For the different applications either of the out-

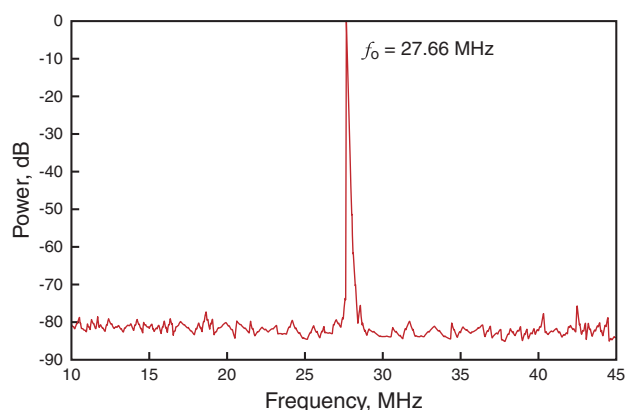


**Figure 2** (online color at [www.lphys.org](http://www.lphys.org)) RF spectrum of the laser ( $f_o$ : central frequency)

put couplers can be chosen as a single output besides the PBS or the PBS can be a single output (see Fig. 8 for an example), and the coupling ratio of the couplers can be changed as well.

The laser consists of the following fibers and fiber optic components, as shown in Fig. 1. A highly doped ytterbium fiber (YbF) is used as the gain media, backward pumped by a 980 nm laser diode via a 980/1030 nm wavelength-division multiplexer (WDM). To investigate the pulse characteristics right behind the gain fiber, a 90/10 splitter (OC<sub>2</sub>) is placed between the WDM and the YbF. The WDM is followed by the semiconductor saturable absorber (SA) that is a commercially available absorber designed for use at around 1020 nm (Batop GmbH, SA-1020-40) and is responsible for the initiation and stabilization of mode-locking. A 10% output port (OC<sub>3</sub>) is included after the SA. The single-mode fiber (SMF) pigtailed between the YbF and the SA are  $\sim 1.9$  m, and the fiber section between the SA and the following PBS is  $\sim 2$  m. The length of these fiber sections is critical in the pulse-shaping mechanism that is based on the spectral broadening in the YbF and the nonlinear polarization evolution in the SMF section [14]. The variation of the polarization state along the spectrum leads to a strong spectral filtering by the PBS. The PBS is followed by a splitter (OC<sub>1</sub>) and an isolator (ISO) realizing the unidirectional cavity. Fiber polarization controllers (PC<sub>1</sub>, PC<sub>2</sub>) are applied on the fiber sections close to the PBS on both sides of it, but the mode-locked operation can be maintained when removing either of them. However, initiation of the mode-locking and adjustment of the desired mode of operation can be easily achieved by rotating the different paddles of the PCs.

## 3. Experimental results

The above described oscillator produces stable mode-locking with low noise (according to the radio-frequency

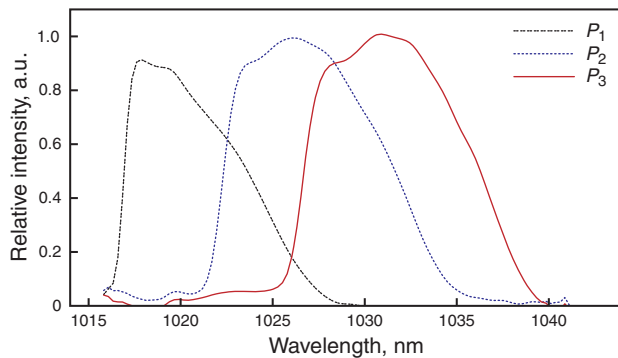


**Figure 3** (online color at [www.lphys.org](http://www.lphys.org)) Tunability of the laser, measured at OC<sub>1</sub> ( $P_{1,2,3}$  refer to different polarization states adjusted by PC<sub>2</sub>)

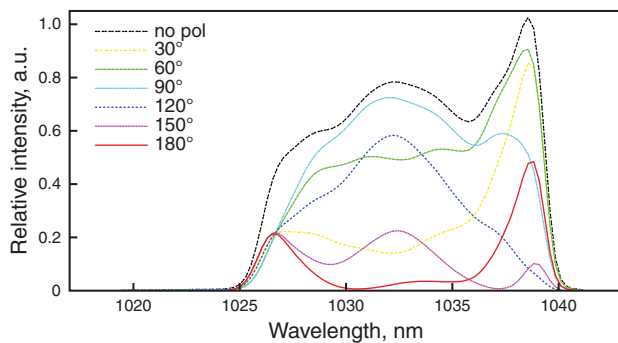


**Figure 4** (online color at [www.lphys.org](http://www.lphys.org)) Spectra measured at different polarizer angles at OC<sub>3</sub>

(RF) spectrum, shown in Fig. 2), and a repetition rate of 27.7 MHz. Besides the initiation of mode-locking the paddles of the PCs are responsible for various effects on the mode of operation. By adjusting the side ( $\lambda/4$ ) paddles the operation can be shifted from noise-like pulses [15] to noisy, Q-switched or cw mode-locking. These can be identified by observing the RF spectra and the autocorrelation functions. The adjustment of PC<sub>2</sub> leads to wavelength tuning of more than 15 nm, as it can be seen in Fig. 3. Furthermore the output coupling ratio of the PBS is most sensitive to the state of the third ( $\lambda/4$ ) paddle of PC<sub>1</sub>. Under some circumstances the spectral width can be increased by increasing the output coupling ratio as well as by increasing the pump power.

The laser operates in the all-normal dispersion regime, where gain, self-phase modulation and dispersion is balanced by spectral (and temporal) filtering. As the output characteristics are extremely sensitive to the settings of the polarization controllers we might conclude that the nonlinear polarization rotation (NPR) together with the polarizer (PBS) has a crucial role in the filtering.

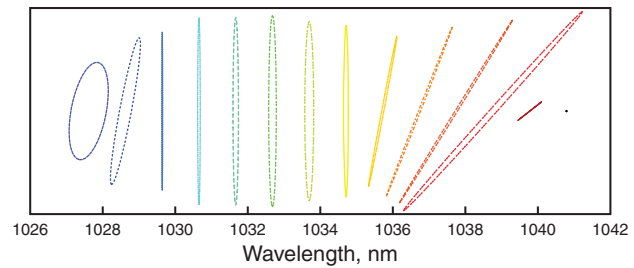


**Figure 5** (online color at [www.lphys.org](http://www.lphys.org)) Polarization states at different wavelengths, measured at OC<sub>3</sub>

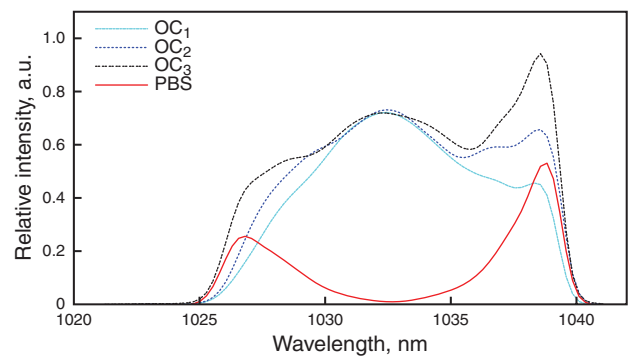


**Figure 6** (online color at [www.lphys.org](http://www.lphys.org)) Spectra measured at the different outputs

In order to observe the effect of the NPR we characterized the polarization state of the laser along the spectrum at OC<sub>3</sub>. This was carried out by measuring the spectra after a polarizer at the output as a function of the polarizer angle. Some of the measured spectra are shown in Fig. 4 and the evaluated polarization states at different wavelengths are plotted in Fig. 5. For stable pulse evolution spectral filtering is required which can be achieved using a PBS. When the polarization is set linear in the middle of the pulse, the PBS affects only the sides of the spectrum. Because of the linear chirping in similariton lasers this filtering leads to temporal pulse-shaping as well. The polarization at the lower wavelength edge of the spectrum is rather circular. This effect is observable at different states of the PCs as well. It is possibly connected to the saturation of the NPR at the tail of the pulse. The polarization at OC<sub>1</sub> is measured to be almost linear and constant along the spectrum.

In order to investigate the laser dynamics the spectral and temporal characteristics of the pulses are measured. The spectra from OC<sub>1</sub> to OC<sub>3</sub> show asymmetric broadening with an increasing peak at the long wavelength edge, as plotted in Fig. 6, possibly due to the higher gain at the leading edge of the propagating chirped pulse. The spectrum at OC<sub>3</sub> is split into the OC<sub>1</sub> and the PBS output spectra according to the polarization state (see the 180° and the 90°

polarizer angle spectra in Fig. 4 for comparison) resulting in a strong modulation of the PBS output spectrum.

The temporal shape of the pulses is characterized by the autocorrelation functions. The width of the autocorrelation functions ( $\Delta T_{AC}$ ) measured at the laser outputs are 10–15 ps and have Gaussian shape except for the one at the PBS output (which looks like the sum of three Gaussians). The output pulses are compressed by a grating pair external to the resonator close to the Fourier-transform limit, implicating a nearly linear chirp. The autocorrelation functions are shown in Fig. 7, plotted with red filled curves. The corresponding spectra are in the insets. Although there is some uncompensated positive third order dispersion, mainly the modulation in the spectra is responsible for the pedestals in the autocorrelation traces. This was verified by comparing the calculated autocorrelation functions of the transform-limited pulse with the chirped and externally compressed pulses, both corresponding to the measured spectra. The calculated autocorrelation functions of the compressed pulses (taking the second and third order dispersion of the cavity and the grating pair into account) are plotted with black lines and the amplitude of the pedestals is similar in the case of transform-limited pulses as well. The pulse widths ( $\Delta T_{pulse}$ ) are estimated from the calculation of the compressed pulses. The shortest pulses are measured at the PBS output, however the quality is poor due to the spectral modulation. It can be seen, that from OC<sub>1</sub> towards the PBS output the spectral width increases and the compressed pulses get narrower as it is expected. Pulses with the highest quality i.e. lowest ratio of power in the pedestals are measured at OC<sub>1</sub>.

In order to obtain a more practical laser the resonator was modified by removing the output couplers (OC<sub>1,2,3</sub>) and the PBS was used as a single output port (see Fig. 8a). In this case  $\sim 0.2$  nJ pulses were measured at the output, which were compressible to  $\sim 195$  fs, with a lower ratio of the energy being in the pedestals as it can be observed in Fig. 8b. The laser had similar characteristics to the above investigated one. The difference is due to the lower resonator loss resulting in lower threshold for cw mode-locking and due to a shorter resonator length ( $f_o = 42.6$  MHz) with weaker NPR. The latter results in a lower contrast in the modulation of the spectrum measured at the PBS leading to higher pulse quality. It is to mention, that the repetition rate can be further increased with this setup.

For most applications amplification of the laser output is necessary. This can be carried out in an all-fiber configuration even at the Yb wavelength by the use of photonic crystal fibers that enable dispersion management [16]. To achieve high pulse quality amplification of a source with unmodulated spectrum would be ideal with further compression. For this reason OC<sub>1</sub> should be maintained as the main output with high pulse quality, unmodulated (parabolic-like) spectrum and linear polarization. Higher pulse energy can be obtained by increasing the output coupling ratio. The PBS output can be used for monitoring.

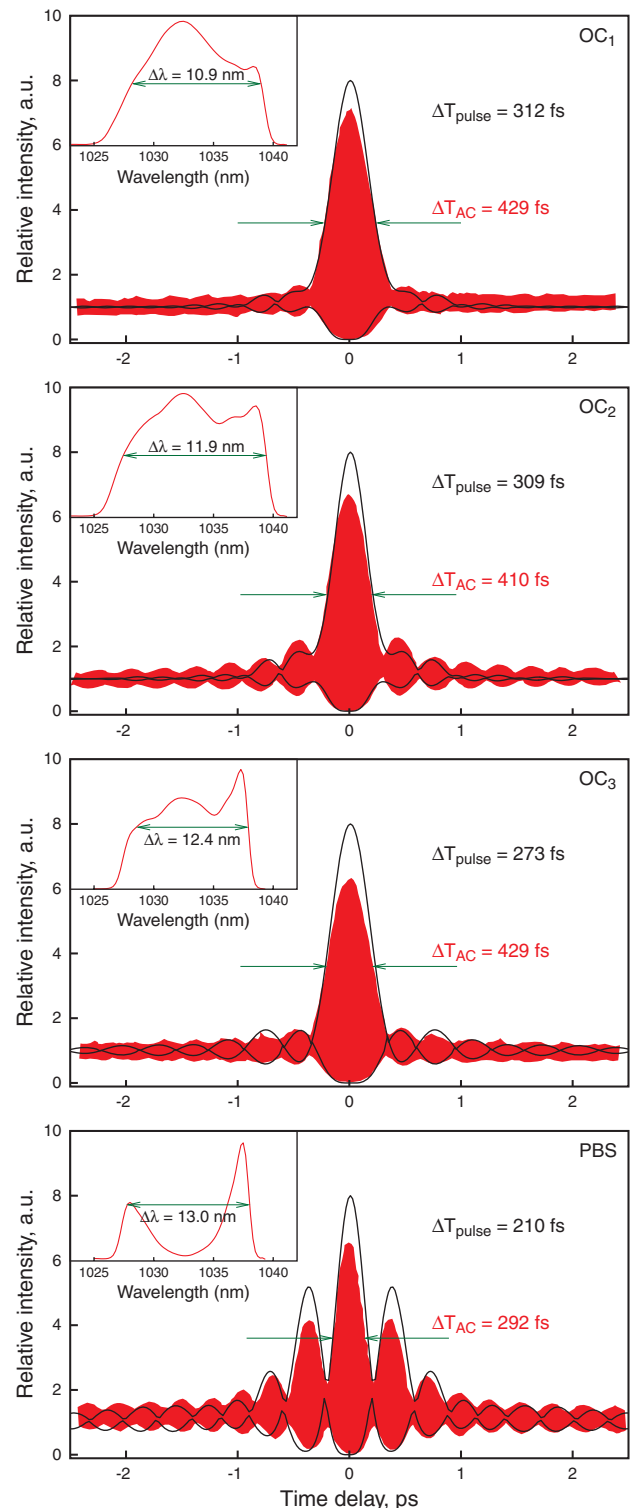


**Figure 7** (online color at [www.lphys.org](http://www.lphys.org)) Measured (red filled curves) and fitted (black lines) autocorrelation functions at the OC<sub>1</sub>, OC<sub>2</sub>, OC<sub>3</sub>, and PBS outputs after external compression by a grating pair.  $\Delta T_{AC}$  is the width of the measured autocorrelation trace,  $\Delta T_{pulse}$  is the estimated pulse width according to the calculations. Insets show the corresponding spectra and spectral widths

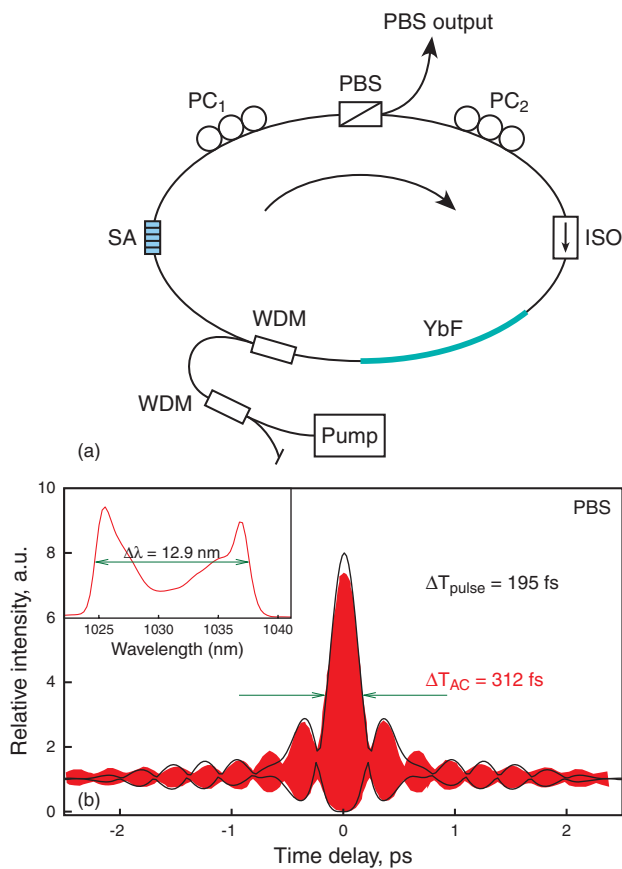


**Figure 8** (online color at [www.lphys.org](http://www.lphys.org)) (a) Experimental setup of a modified oscillator with a single output (PBS rejection port) and (b) measured (red filled curves) and fitted (black lines) auto-correlation functions with the spectrum in the inset

## 4. Conclusion

We have demonstrated an all-fiber Yb ring oscillator without any intra-cavity dispersion compensation with four output ports that were compared. The broadest spectrum was measured at the PBS rejection port but it was strongly modulated. Other spectra at the 90/10 splitter outputs had more parabolic-like shape. The autocorrelation widths at all outputs are  $\sim 10$ – $15$  ps and the pulses can be compressed close to the Fourier-transform limit by a grating

pair. The shortest compressed pulses are 210 fs, and the RF spectrum as well as the pulse train observed on an oscilloscope showed stable cw mode-locking with a high S/N ratio. Furthermore, a shorter oscillator was presented to show similar characteristics. The oscillator with a single PBS rejection port generated pulses compressible to as short as 195 fs with a relatively high pulse quality.

*Acknowledgements* This research was supported by the Hungarian National Grant No. NKFP1-0007/2005.

## References

- [1] C. Fortier, B. Kibler, J. Fatome, C. Finot, S. Pitois, and G. Millot, *Laser Phys. Lett.* **5**, 817–820 (2008).
- [2] Yu.O. Barmenkov, J.L. Cruz, and M.V. Andres, *Laser Phys. Lett.* **5**, 676–679 (2008).
- [3] M. Delgado-Pinar, A. Díez, J.L. Cruz, and M.V. Andrés, *Laser Phys. Lett.* **5**, 135–138 (2008).
- [4] J.R. Buckley, F.W. Wise, F.Ö. Ilday, and T. Sosnowski, *Opt. Lett.* **30**, 1888–1890 (2005).
- [5] V. Cautaerts, D.J. Richardson, R. Paschotta, and D.C. Hanna, *Opt. Lett.* **22**, 316–318 (1997).
- [6] A. Ruehl, O. Prochnow, M. Engelbrecht, D. Wandt, and D. Kracht, *Opt. Lett.* **32**, 1084–1086 (2007).
- [7] J.W. Nicholson, S. Ramachandran, and S. Ghalmi, *Opt. Express* **15**, 6623–6628 (2007).
- [8] O. Katz, Yo. Sintov, Ye. Nafcha, and Ya. Glick, *Opt. Commun.* **269**, 156–165 (2007).
- [9] A. Chong, J. Buckley, W. Renninger, and F. Wise, *Opt. Express* **14**, 10095–10100 (2006).
- [10] C.K. Nielsen and S.R. Keiding, *Opt. Lett.* **32**, 1474–1476 (2007).
- [11] R. Herda and O.G. Okhotnikov, *IEEE J. Quantum Electron.* **40**, 893–899 (2004).
- [12] O. Prochnow, A. Ruehl, M. Schultz, D. Wandt, D. Kracht, *Opt. Express* **15**, 6889–6893 (2007).
- [13] K. Kieu and F.W. Wise, *Opt. Express* **16**, 11453–11458 (2008).
- [14] A. Ruehl, D. Wandt, U. Morgner, D. Kracht, *Opt. Express* **16**, 8181–8189 (2008).
- [15] M. Horowitz, Y. Barad, and Y. Silberberg, *Opt. Lett.* **22**, 799–801 (1997).
- [16] B.-W. Liu, M.-L. Hu, X.-H. Fang, Y.-Z. Wu, Y.-J. Song, L. Chai, C.-Y. Wang, and A.M. Zheltikov, *Laser Phys. Lett.* **6**, 44 (2009).